



# Design principles for noninvasive, longitudinal and quantitative cell tracking with nanoparticle-based CT imaging

Rinat Meir, MSc<sup>a,1</sup>, Oshra Betzer, MSc<sup>a,b,1</sup>, Menachem Motiei, PhD<sup>a</sup>, Noam Kronfeld, PhD<sup>c</sup>, Chaya Brodie, PhD<sup>c,d</sup>, Rachela Popovtzer, PhD<sup>a,\*</sup>

<sup>a</sup>Faculty of Engineering and the Institute of Nanotechnology and Advanced Materials, Bar-Ilan University, Ramat Gan, Israel

<sup>b</sup>Gonda Brain Research Center, Bar-Ilan University, Ramat Gan, Israel

<sup>c</sup>The Goodman Faculty of Life Sciences, Bar-Ilan University, Ramat-Gan, Israel

<sup>d</sup>Hermelin Brain Tumor Center, Department of Neurosurgery, Henry Ford Hospital, Detroit, MI, USA

Received 19 June 2016; accepted 22 September 2016

## Abstract

Contradictory results in clinical trials are preventing the advancement and implementation of cell-based therapy. To explain such results, there is a need to uncover the mystery regarding the fate of the transplanted cells. To answer this need, we developed a technique for noninvasive *in vivo* cell tracking, which uses gold nanoparticles as contrast agents for CT imaging. Herein, we investigate the design principles of this technique for intramuscular transplantation of therapeutic cells. Longitudinal studies were performed, displaying the ability to track cells over long periods of time. As few as 500 cells could be detected and a way to quantify the number of cells visualized by CT was demonstrated. Moreover, monitoring of cell functionality was demonstrated on a mouse model of Duchenne muscular dystrophy. This cell-tracking technology has the potential to become an essential tool in pre-clinical as well as clinical trials and to advance the future of cell therapy.

© 2016 Elsevier Inc. All rights reserved.

**Key words:** Cell tracking; Cell therapy; Nanoparticles; Computed tomography; Imaging

Cell therapy provides a promising approach for diseases and injuries that conventional therapies cannot cure effectively.<sup>1</sup> In particular, stem cells, with the potential to regenerate injured tissue, have broad applicability in fields such as oncology, cardiology, neurology and muscle regeneration.<sup>2–5</sup> To achieve their therapeutic potential, these cells must home to the site of

injury, differentiate into the target cells, survive, and engraft after transplantation.<sup>6</sup> Therefore, the use of therapeutic cells has been widely investigated in preclinical studies as well as in human clinical trials.<sup>7</sup>

However, contradictory results in recent clinical trials are a major obstacle in the advancement and implementation of cell therapy.<sup>8</sup> While some patients demonstrate a significant improvement, others show minimal to no improvement after cell therapy. *In vivo* cell tracking is needed to elucidate essential knowledge regarding fundamental trafficking patterns and poorly-understood mechanisms underlying the success or failure of cell therapy.<sup>9–13</sup> Various methods, such as optical imaging,<sup>14–16</sup> ultrasound,<sup>17</sup> positron emission tomography (PET)<sup>18</sup> and magnetic resonance imaging (MRI)<sup>19,20</sup> attempt to perform such tracking and imaging, but an optimal solution for the challenge of cell tracking does not yet exist.

We have recently demonstrated a novel noninvasive cell tracking technique which combines the use of gold nanoparticles (GNPs) as contrast agents and computed tomography (CT) as an imaging modality.<sup>21–23</sup> GNPs are biocompatible and have

**Abbreviations:** PET, positron emission tomography; MRI, magnetic resonance imaging; CT, computed tomography; GNPs, gold nanoparticles; UV–vis, ultraviolet–visible spectroscopy; FAAS, flame atomic absorption spectroscopy.

The authors have declared that no competing interest exists.

**Funding:** This work was partially supported by the Israeli Ministry of Science, Technology & Space and by the ADI foundation, and by the Ministry of Science, Technology & Space doctoral scholarship for Rinat Meir and Oshra Betzer.

\*Corresponding author at: Faculty of Engineering and the Institute of Nanotechnology and Advanced Materials, Bar-Ilan University, Ramat Gan, Israel.

*E-mail address:* rachela.popovtzer@gmail.com (R. Popovtzer).

<sup>1</sup> Authors contributed equally to this work

unique physical and chemical properties,<sup>24–29</sup> making them attractive contrast agents for several imaging modalities.<sup>17,18,30–34</sup> Specifically, the high atomic number of gold can induce strong x-ray attenuation, which makes GNPs ideal contrast agents for CT, which is one of the leading radiology technologies applied in the field of biomedical imaging. CT is characterized by high temporal and spatial resolution, and it is among the most convenient imaging tools used in hospitals to date, in terms of availability, efficiency, and cost. Thus, we chose to explore the marriage between GNPs and CT imaging for the purpose of noninvasive cell tracking and we termed our technique CT<sup>3</sup> – computed tomography of cell tracking in cell therapy.

Lately, we have applied the CT<sup>3</sup> technology for noninvasive monitoring of mesenchymal stem cells transplanted in a rat model for depression,<sup>22</sup> and for cancer immunotherapy treatment with cancer-specific T cells.<sup>21</sup> In addition, we performed excessive *in vitro* studies in order to optimize the balance between the need to maintain the therapeutic abilities of the injected cells while receiving maximum cell loading in order to achieve sufficient contrast for *in vivo* observation of cells by CT.<sup>23</sup>

Cells transplantation is performed by several routes of administration, including intravenous, intrastriatal, subcutaneous and intramuscular administration. Cell bio-distribution and imaging abilities for cell tracking vary from one route to the other; therefore, in this study we chose to focus on intramuscular administration which is a common route of administration used in stem cell therapy.<sup>17,35–37</sup>

The goal of this research was to establish design principles for our CT<sup>3</sup> technology: to show our ability of longitudinal cell tracking over the course of several weeks, to determine the detection limit of CT<sup>3</sup> in term of the smallest number of cells injected that can be detected and to provide a mathematical model for quantifying the number of cells visualized.

In addition, in our previous work<sup>23</sup> cell functionality post labeling was extensively studied *in vitro*. Thus, there was a need to further validate *in vivo* the retention of cell functionality post intramuscular transplantation.

## Methods

### *GNPs synthesis and conjugation*

#### *Synthesis*

GNPs were prepared using sodium citrate according to the known methodology described by Enustun and Turkevich.<sup>38</sup> 0.414 mL of 1.4 M HAuCl<sub>4</sub> solution in 200 mL water was added to a 250 mL single-neck round bottom flask and stirred in an oil bath on a hot plate until boiled. 4.04 mL of a 10% sodium citrate solution (0.39 M sodium citrate tribasic dihydrate 98%, Sigma cas 6132-04-3) was then quickly added. The solution was stirred for 5 min, and then the flask was removed from the hot oil and placed aside until cooled.

#### *Conjugation*

In order to prevent aggregation and stabilize the particles in physiological solutions, *O*-(2-Carboxyethyl)-*O'*-(2-mercaptoethyl) heptaethylene glycol (PEG7) (95%, Sigma-Aldrich, Israel Ltd.) was

absorbed onto the GNPs. This layer also provides the chemical groups required for antibody conjugation (–COOH). First, the solution was centrifuged to dispose of excess citrate. PEG7 solution was then added to the GNPs solution, stirred overnight and put in a centrifuge in order to dispose of excess PEG. Next, with the purpose of increasing cell-uptake rate, stabilized GNPs were further coated with glucose. Excess EDC (N-ethyl-N-(3-dimethylaminopropyl) carbodiimide) and NHS (N-hydroxysuccinimide) (Thermo Fisher Scientific, Inc., Rockford, IL) were added to the solution, followed by addition of Glucose-2 (2GF)(D-(+)-Glucosamine hydrochloride, Sigma-Aldrich, Israel Ltd.). NHS and EDC form an active ester intermediate with the –COOH functional groups, which can then undergo an amidation reaction with the glucose –NH<sub>2</sub> group. Glucosamine molecule C-2 (2GF-GNP): D-(+)-Glucosamine hydrochloride (3 mg; Sigma Aldrich) was added to the activated linker-coated GNPs.

#### *Characterization*

Transmission electron microscopy (TEM, JEM-1400, JEOL) was used to measure the size and shape of the GNPs, which were further characterized using ultraviolet–visible spectroscopy (UV–Vis; UV-1650 PC; Shimadzu Corporation, Kyoto, Japan) following each level of coating.

#### *Labeling cells with GNPs*

##### *Human mesenchymal stem cells ADSI (hMSCs) isolation and expansion*

hMSCs were isolated from adult human subcutaneous adipose tissue, as previously described.<sup>22</sup> The cells were plated in T-225 tissue culture flasks (Corning, Corning, NY) and cultured with mesenchymal stem cell growth medium and preadipocyte growth medium (Cambrex Bio Science), respectively, at 37 °C in 5% CO<sub>2</sub> and 90% humidity. The medium was changed every 3 days.

#### *Cell uploading with GNPs*

Stem cells were cultured in 5 ml glucose-free DMEM medium containing 5% FCS, 0.5% penicillin and 0.5% glutamine. Cells were centrifuged and a saline solution containing GNPs was added in excess. The cells were then incubated at 37 °C for 2 hours. After incubation, the cells were centrifuged twice (7 minutes in 1000 rpm) to wash out unbound nanoparticles.

#### *Flame gold analysis*

For analyzing the average amount of GNPs within the cells before each *in vivo* experiment cells were incubated with GNPs (30 mg/mL) for 2 h. The uptake was analyzed using Flame Atomic Absorption Spectroscopy (FAAS, SpectrAA140, Agilent Technologies). The cells were melted with aqua-regia acid, a mixture of nitric acid and hydrochloric acid in a volume ratio of 1:3. The samples were then evaporated, filtered and diluted to a final volume of 10 mL. Au lamp was used in order to determine the gold concentration in the samples. Gold concentration in each sample was determined according to its absorbance value with correlation to a calibration curve. Each sample was analyzed in triplicate and averages and standard deviations were taken.

### *In vivo experiments*

To explore the longitudinal abilities of CT<sup>3</sup>, mesenchymal stem cells ( $2 \times 10^6$ ) were incubated with GNPs and then intramuscularly injected in the limbs of 5 mice. Cells were injected in a fixed volume of 20  $\mu$ l. The mice were scanned using a micro-CT, 24 hours post cell's transplantation, and once a week for four weeks.

To determine detection abilities: mesenchymal stem cells were loaded with GNPs and three different cell amounts ( $10 \times 10^5$ ,  $5 \times 10^5$  and  $2 \times 10^5$ ) and injected in a fixed volume of 20  $\mu$ l intramuscularly to the limbs of 10 mice. The mice were CT-scanned 48 hours post injection. To validate the limit of detection: mice were injected with different amounts of cells ranging from 50,000 cells to 500 cells ( $50 \times 10^3$ ,  $30 \times 10^3$ ,  $10 \times 10^3$ ,  $8 \times 10^3$ ,  $5 \times 10^3$ ,  $2 \times 10^3$ ,  $1 \times 10^3$ ,  $0.5 \times 10^3$ ) in a fixed volume of 20  $\mu$ l. Images were obtained 48 hours post injection by using a micro-CT device and the projection images were reconstructed into cross sectional slices.

For cell functionality studies mdx mouse model was used. Mice were injected with gold-labeled hMSCs and CT-scanned once a week for one month.

### *In vivo micro-CT scans*

*In vivo* scans of the injected regions were performed using a micro-CT scanner (Skyscan High Resolution Model 1176) with a nominal resolution of 35  $\mu$ m, a 0.2 mm aluminum filter, and a tube voltage of 45 kV. Reconstruction was done with a modified Feldkamp<sup>39</sup> algorithm using the SkyScanNRecon software accelerated by GPU.<sup>40</sup> Ring artifact reduction, Gaussian smoothing (3%), and beam hardening correction (20%) were applied. Two dimensional images and quantitative measurements were obtained using CT-Analyze ("CT-An") software. Volume rendered three-dimensional (3D) images were generated using an RGBA transfer function in both SkyScan CT-Volume ("CTVol") and CT-Voxel ("CTVox") softwares.

### *Animal care*

All experimental procedures and methods were approved by the Animal Care Committee of Bar-Ilan University and in accordance with the National Institutes of Health guidelines and regulations. For cell functionality *in vivo* studies, MDX mice of 6-8 weeks old weighing 25-30 g were used for this study. Mice were housed in stainless steel cages in groups of four under standard environmental conditions ( $23 \pm 1$  °C,  $55 \pm 5\%$  humidity and a 12/12 h light/dark cycle) and maintained with free access to water and a standard laboratory diet (carbohydrates 30%; proteins 22%; lipids 12%; vitamins 3%).

## **Results**

### *Cell labeling with GNPs for noninvasive cell tracking*

In order to obtain visibility of transplanted cells by noninvasive *in vivo* CT imaging, cells were labeled with GNPs *in vitro* prior to cell implantation. For that purpose, GNPs (20 nm diameter) were synthesized and coated with PEG for

stability and then with glucose according to our previously published protocol (Figure 1).<sup>21–23</sup> Then, we examined the feasibility of the uptake of GNPs by the cells; mesenchymal stem cells were incubated with the GNPs for 2 hours, the average amount of GNPs uptake was analyzed using Flame Atomic Absorption Spectroscopy (FAAS), and as previously described<sup>22</sup> was found to be 1.1 million particles per cell (std: 0.12) ( $8.8 \times 10^{-8}$  mg gold per cell). Efficiency of cell labeling was further demonstrated by microscopy images (Figure 1, D).

### *The ability to image cells over time*

An important aspect in cell tracking is the ability to trace the cells over long periods of time, as the migration and homing abilities of therapeutic cells to the site of injury are some of the most interesting questions on the field of cell therapy. To explore the longitudinal abilities of CT<sup>3</sup>, mesenchymal stem cells ( $2 \times 10^6$ ) were incubated with GNPs and then intramuscularly injected in the limbs of mice. 24 hours post injection the mice were scanned in a micro-CT device. In order to see whether the signal changes over time we continued to scan the mice once a week for up to 4 weeks post injection.

The results of this longitudinal imaging experiment are presented in Figure 2. 24 hours after injection, a strong signal was observed at the site of injection. This is due to the fact that the cells injected were uploaded with GNPs providing a good contrast for the CT. After this time point there is a very clear trend over time: the volume of the labeled-cells becomes smaller while the signal intensity increases. This could indicate that the cells migrate to form clusters over time.

These results demonstrate that there is no loss in signal over time and we were able to track the 'golden cells' for 4 weeks. Moreover, Figure 2 also presents another important advantage for clinical applications – the ability to view the CT imaging results in different perspectives, such as two-dimensional (2D) cross-sectional slices or three-dimensional (3D) volume rendering images.

### *Determining the limit of detection*

In many cell therapy studies, several hundred thousand cells are transplanted<sup>22,33</sup>; thus the imaging abilities of this magnitude of cells were initially evaluated. For this purpose, mesenchymal stem cells were loaded with GNPs and three different cell amounts ( $10 \times 10^5$ ,  $5 \times 10^5$  and  $2 \times 10^5$ ) were injected intramuscularly to the limbs of mice. 48 hours post injection the mice were CT-scanned. As shown in Figure 3, a very strong signal was detected in all three cell-quantities and it was clear that even smaller amounts of cells could also be detected.

In order to answer important questions regarding the behavior, migration and fate of cells, there is a need to image much smaller numbers of cells within the body. We decided to determine the detection limit of CT<sup>3</sup> and to answer the question: what is the smallest number of cells injected in the muscle that could be detected?

To find the detection limit of CT<sup>3</sup> we conducted a follow-up experiment with small numbers of cells. In this experiment, 10 mice were injected with different amounts of cells ranging from 50,000 cells to 500 cells. Images were obtained 48 hours post

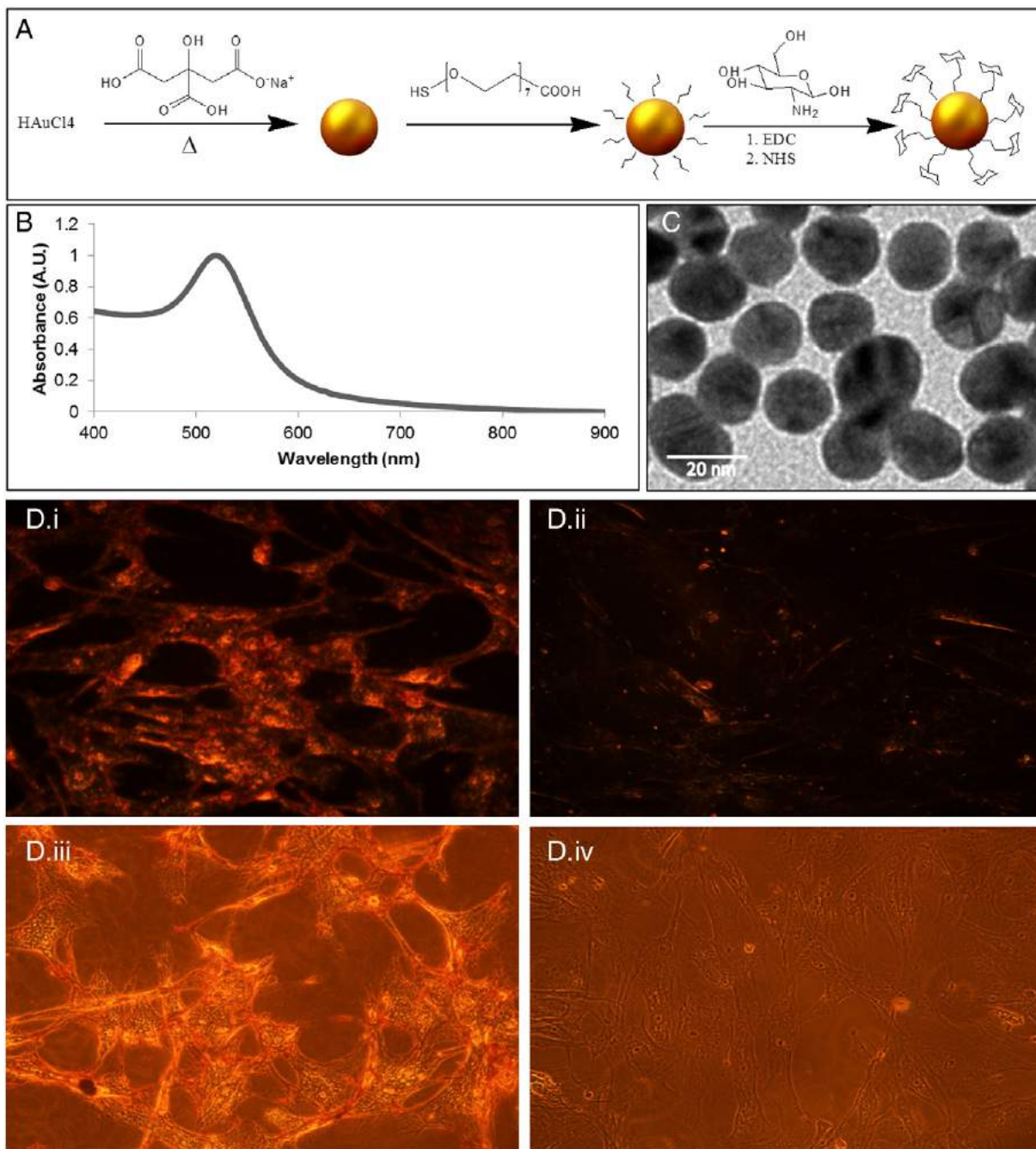


Figure 1. GNPs synthesis and microscopy images of GNP-labeled cells. **(A)** Schematic diagram of the GNPs synthesis process: GNPs were conjugated to the linker polyethylene glycol (PEG), followed by covalent conjugation to glucose. **(B)** Transmission electron microscopy image of 20 nm GNPs. **(C)** Optical properties of the GNPs as assessed by ultraviolet–visible spectroscopy. **(D)** Dark field and bright field images of mesenchymal stem cells labeled with GNPs. i. Darkfield after incubation with GNPs. ii. Darkfield before incubation with GNPs. iii. Brightfield after incubation with GNPs. iv. Brightfield before incubation with GNPs.

injection by using a micro-CT device. Figure 4 displays representative 2D images of 50,000, 5000 and 500 cells resulting from the CT scans. Remarkably, due to the presence of the gold inside the cells a strong signal was observed at the injection site for as low as 500 cells. Less than 500 cells could not be detected thus the detection limit was set to 500 cells.

#### Quantitative cell tracking

As demonstrated in Figure 4, when following a fixed GNP-labeling protocol, the obtained intensity of the CT signal is a direct result of the amount of cells injected. This means that by using basic image analysis tools, quantification of the number

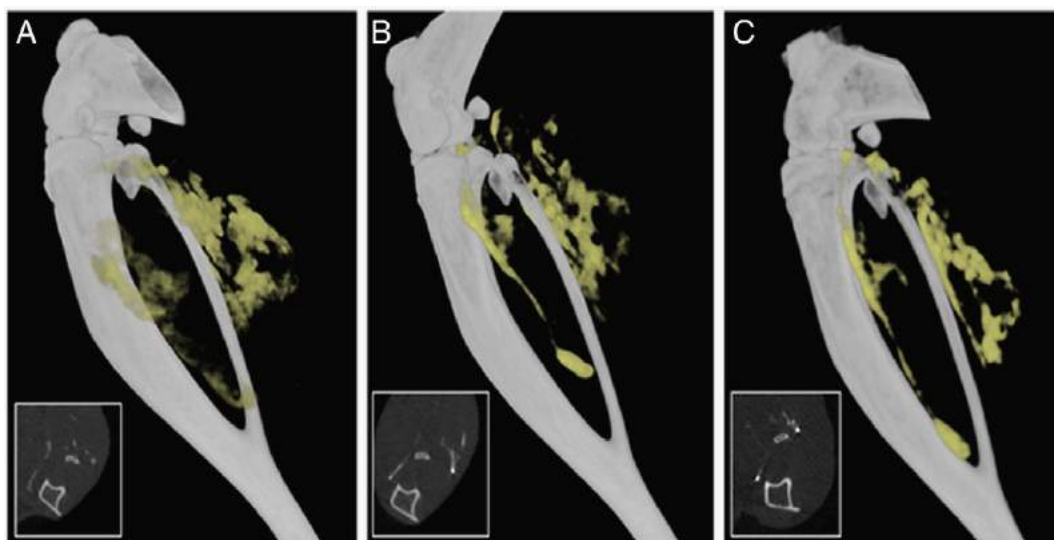


Figure 2. Longitudinal cell tracking with CT<sup>3</sup>. 3D volume rendering of CT scans of cells after transplantation of  $2 \times 10^6$  mesenchymal stem cells in the muscle of the mouse limb (A) 24 hours (B) 2 weeks (C) 4 weeks post injection. Inset: 2D cross-sectional slices showing the signal in the muscle.

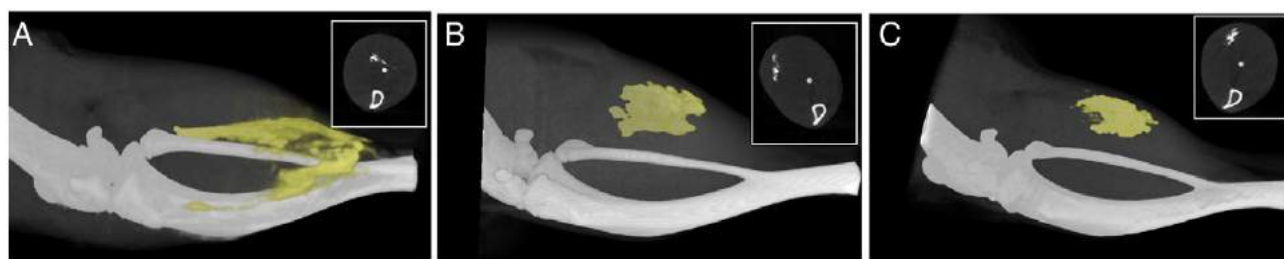


Figure 3. CT images of ‘golden cells’ injected in three different quantities. 3D volume rendering of CT images obtained two days post injection, (A)  $10 \times 10^5$  cells, (B)  $5 \times 10^5$  cells, (C)  $20 \times 10^5$  cells. Inset: 2D cross-sectional slices.

of cells in the muscle is feasible. The CT images obtained in the experiment from 8 different cell amounts (500–50,000 cells) were analyzed and were used to calculate three important parameters: the number of voxels containing gold, the mean density within these voxels and the maximum gray value within these voxels. ‘CT value’ was modeled by the following equation:

$$\text{CT value} = \text{intensity} * \text{number of voxels}$$

$$\text{Intensity} = a \times \text{mean} + (1-a) \times \text{maxgray value}$$

The parameter ‘a’ was set to be 0.95, as the contribution of the maximum gray value to the intensity is much less significant than the mean gray value of the area containing gold.

Figure 5 presents the results of plotting the number of cells as a function of the ‘CT value.’ A linear trend is displayed with a linear equation that allows receiving the number of cells from the calculated ‘CT value.’

$$\text{Number of cells} = 0.0298 \times \text{CT value} + 426.9$$

The equation was tested on several scans and was able to predict the number of cells in the images obtained. The number

426.9 represents the theoretical minimum number of cells detected and is approximately equal to the experimental detection limit of 500 cells. The importance of such quantification is that the fate of the injected cell could be monitored in accurate numbers and details.

Additional analysis and quantification were performed for the images obtained over time in the longitudinal cell tracking experiments. As described above, mesenchymal stem cells were injected and scanned over a period of four weeks. For these images we analyzed two parameters separately: number of voxels containing gold and the mean gray value for these voxels. Figure 6 demonstrates that over time these two parameters exhibit opposite trends: while the mean gray value increases, the number of voxels containing gold decreases. This trend indicates that over time the cells form clusters and come closer together resulting in a stronger and denser signal.

#### *Validation of cell functionality in vivo and simultaneous monitoring of recovery*

Once establishing the ability for longitudinal, sensitive and quantitative cell tracking by noninvasive CT<sup>3</sup>, we were interested in validating that cell functionality is retained post GNP-labeling and

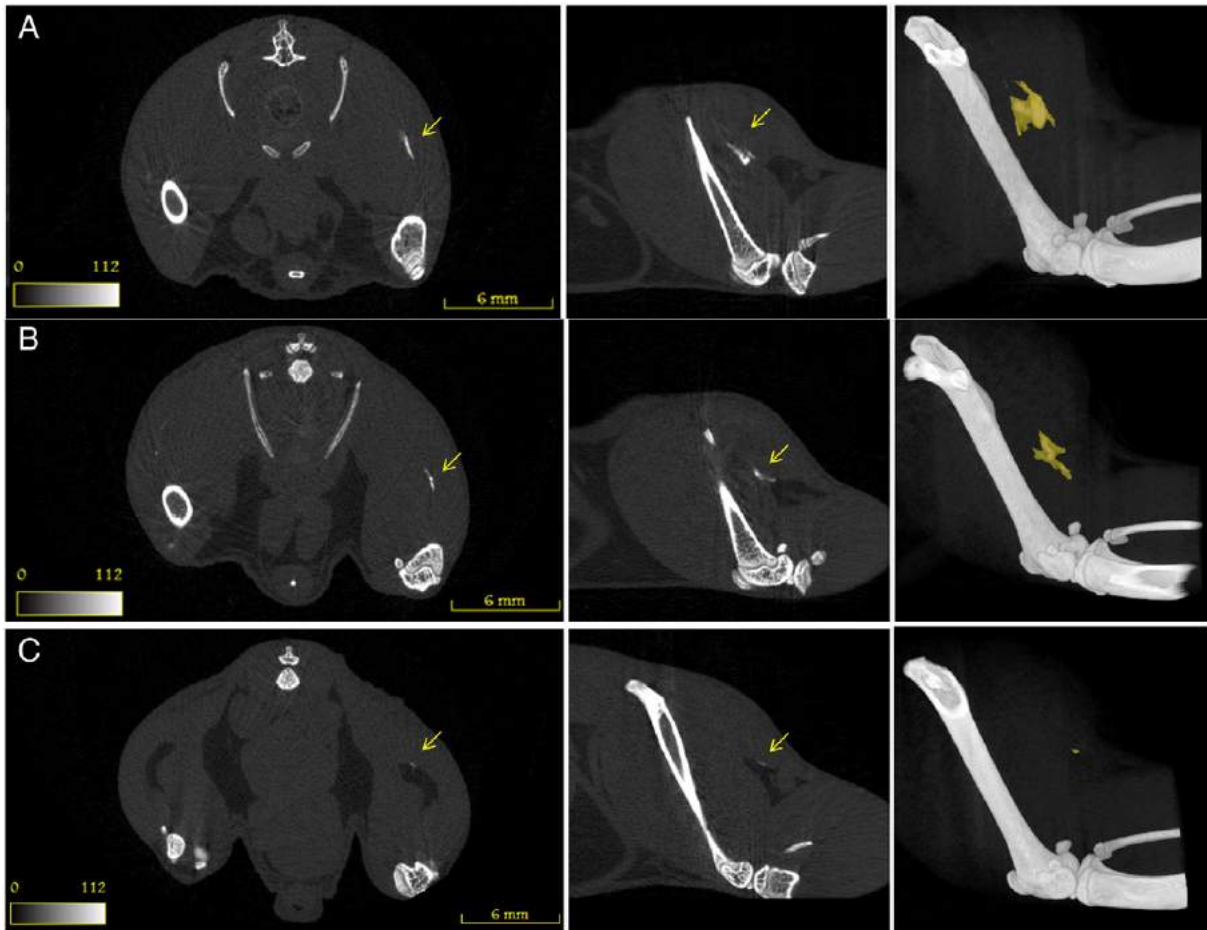


Figure 4. Detection limit of CT for imaging 'golden cells.' Left: transverse 2D slices. Center: sagittal 2D slices. Right: 3D volume rendering. (A) 50,000 cells (B) 5000 cells. (C) 500 cells. Yellow arrows indicate the site of injection.

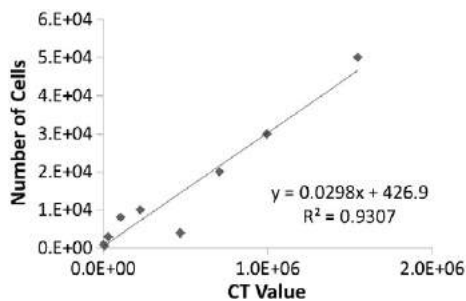


Figure 5. Number of cells as a function of the CT value. Quantitating CT value of 'golden cells' injected to 8 mice in different quantities. The CT value is:  $(0.95 \times \text{mean} + 0.05 \times \text{max}) \times \text{volume}$ . The number 426.9 in the resulting linear equation is in fact the calculated detection limit of our tracking technology.

that the GNPs do not harm the therapeutic abilities of the cells. For this purpose mesenchymal stem cells loaded with GNPs were transplanted in the MDX mouse model. MDX is the most widely used model for Duchenne muscular dystrophy, a disorder which results in muscle degeneration and premature death. Mesenchymal stem cells have been shown to migrate to sites of injury and inflammation and exert therapeutic effects in various disorders including Duchenne muscular dystrophy.<sup>4,41–43</sup>

Herein, mesenchymal stem cells ( $1 \times 10^6$ ) were labeled with GNPs and injected into the limb of MDX mice. CT scans were performed once a week over a period of one month post injection. Figure 7 presents longitudinal 3D images of the 'golden cells.' The cells were well detected and imaged over time and it appears that with time the cells are migrating from the injection site and are spreading in the muscle.

Besides the ability for noninvasive, quantitative and longitudinal tracking of GNP-labeled cells, in the case of Duchenne muscular dystrophy the use of CT offers the major advantage of simultaneously monitoring the progression of the muscle disease. Ectopic calcification is a pathologic deposition of calcium salts in the muscle tissues and is a characteristic feature of muscular pathology. Calcification of the skeletal muscle has been reported to occur in the mdx mouse model for Duchenne muscular dystrophy.<sup>44</sup> As previously demonstrated by Kikkawa et al due to the high density of the calcification particles, ectopic calcification can be observed clearly using CT.<sup>45</sup>

Thus CT<sup>3</sup> is an attractive tool for cell tracking after cell treatment of Duchenne muscular dystrophy as indeed demonstrated in Figure 8. Figure 8, A presents the 3D scan of the mouse limbs two weeks post transplantation of labeled mesenchymal stem cells. In yellow are the GNP-labeled cells injected locally in the

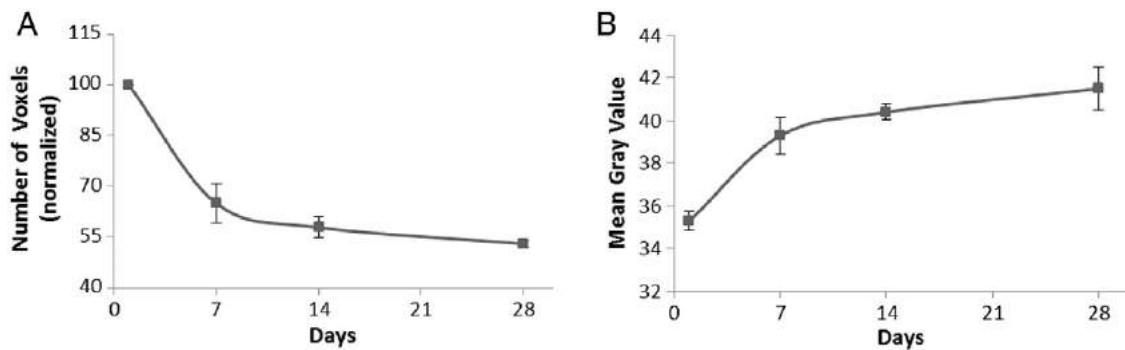


Figure 6. Quantitative analysis of longitudinal cell tracking. CT analysis of number of voxels and mean gray value as they change over time: (A) number of gold voxels normalized. (B) mean gray value of gold voxels. The volume of the GNP-labeled MSCs decreases while average density increases.

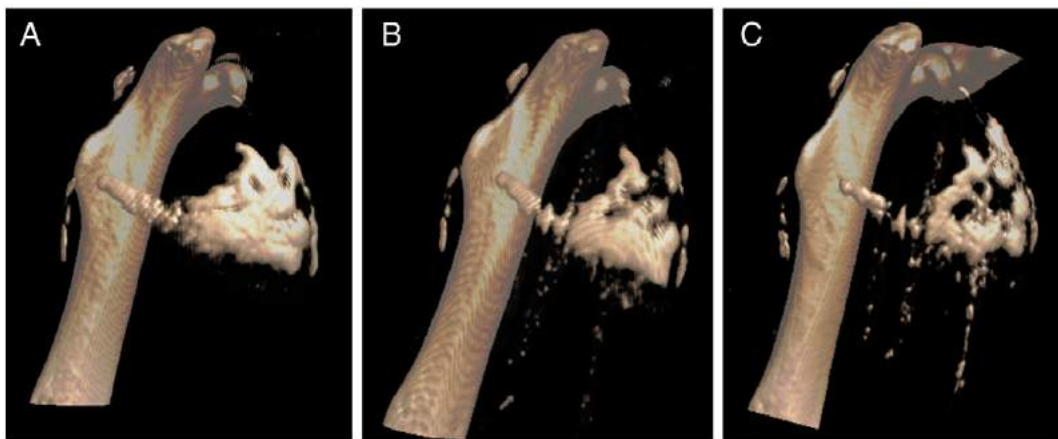


Figure 7. Longitudinal CT imaging of ‘golden cells’ in MDX mouse. (A) 1 week (B) 2 weeks (C) 4 weeks post injection. Cells were injected to the thigh muscle and monitored for 4 weeks. Images demonstrate migration of cells.

right limb. In bright blue is the calcification observed. Figure 8, B is a sagittal slice of the same scan. It is simple to distinguish between the bones (gray value 121), the calcification (gray value 58) and the GNP-labeled cells (gray value 252). There is a clear difference in calcification between the two limbs. While the untreated limb has high calcification, the treated limb has very low calcification. Figure 8, C is a 3D image of the control, an untreated MDX mouse. Here, the calcification is visualized in both limbs.

Thus, Figure 8, A presents how CT simultaneously visualizes the golden mesenchymal stem cells at the injection site, and a significant change in the appearance of the muscle that results from changes in the state of calcification that is observed only at the treated limb, indicating a local therapeutic effect. Importantly, limbs of normal mice did not show this calcification signal that is characteristics of the MDX mice (data not shown). This is an *in vivo* validation that the cells maintain their functionality post GNP-labeling, making CT<sup>3</sup> an ideal technology for cell tracking in cell therapy.

## Discussion

CT<sup>3</sup> – computed tomography of cell tracking in cell therapy – is our noninvasive cell tracking technique which combines the use of GNPs as a contrast agent and CT as an imaging modality.

The ability to trace cells over long periods of time is one of the most important needs in the field of cell therapy. Thus, the goal of this research was to establish design principles for cell tracking using CT, when utilized for intramuscular cell transplantation. Longitudinal cell tracking was performed, with no loss in signal over time. This is a unique ability of CT<sup>3</sup> and is attributed to the presence of the GNPs in the cells. We were able to track the ‘golden cells’ for 4 weeks. The images revealed that over time the cells tend to form clusters and come closer together, resulting in a stronger and denser CT signal.

In our experiments, the minimum detection limit, in terms of the smallest number of cells detected was determined to be 500 cells. This is a remarkable result which will enable tracking of very small clusters of cells post transplantation. However, it should be noted that the ability to image such a small number of cell is only possible when the cells are injected intramuscularly. In this mode of injection the cells are injected locally and are very close together which results in the strong detectable signal. Any other mode of injection would result in a much higher detection limit.

In addition, a mathematical model for quantifying the number of cells visualized in the CT images was provided. We were able to generate an equation which provides the number of cells as a function of the CT value obtained. The significance of such quantification is that the fate of the injected cell could be monitored

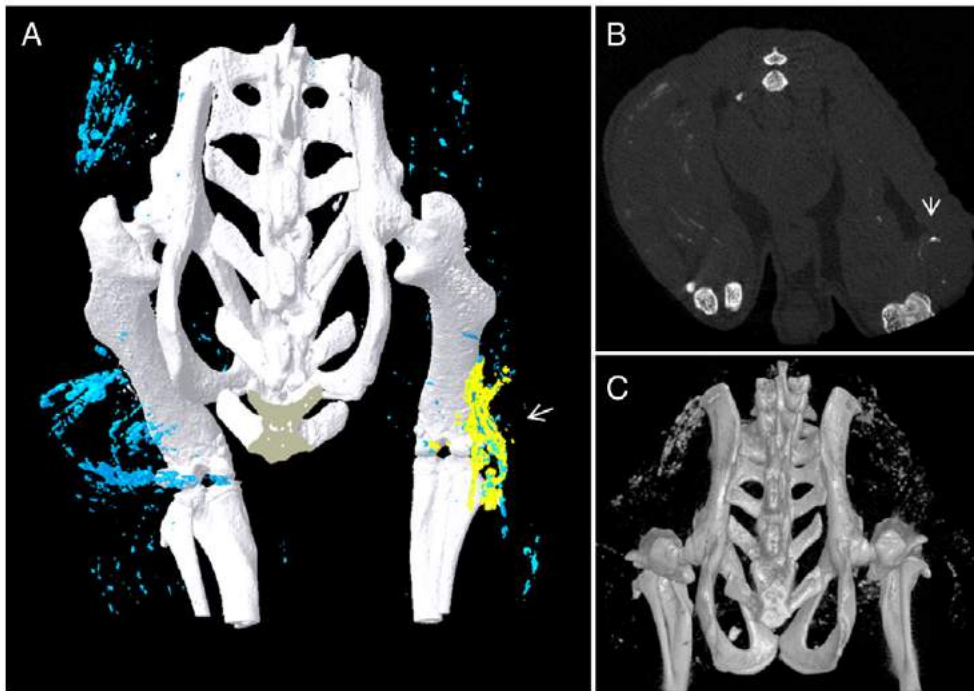


Figure 8. Validation of cell functionality and simultaneous monitoring of muscle recovery: imaging cell treatment of muscle in MDX mouse. **(A)** 3D volume rendered CT scan demonstration of mouse two weeks post transplantation in the right limb, arrow indicating injection site. Yellow-GNPs located in the injection site, blue-calcification, mainly in the untreated left limb. Calcification is much greater in the untreated leg than in the treated leg. **(B)** 2D cross-sectional slice. **(C)** An untreated MDX mouse; calcification signal is observed in both limbs.

in details and this will enable answering questions regarding the percentage of cells that migrate and home to the site of injury.

One of the greatest concerns in longitudinal imaging with nanoparticles is whether the imaged cells are still alive over time. This concern, previously addressed in our *in vitro* and *in vivo* studies,<sup>21–23</sup> is of great importance and justifies further *in vivo* confirmation. For this purpose, studies were performed on the MDX mouse model with mesenchymal stem cell therapy. We were able to track the injected cells over time, and at the same time monitor muscle recovery due to the anatomical abilities of CT. Two weeks post injection local recovery was observed in the muscle in which golden mesenchymal stem cells were transplanted and imaged, thus proving functionality of the injected cells.

The ability to track the small clusters of cells over time is a crucial need in cell tracking, as the migration and homing abilities of cells to the site of injury is one of the most interesting questions on the field of cell therapy. With longitudinal CT<sup>3</sup> such questions could be answered and thus impact the future of cell therapy. We expect that the remarkable capabilities of CT<sup>3</sup> to enable noninvasive, quantitative and longitudinal cell tracking, with simultaneous monitoring of symptoms and recovery will generate an overall real-time assessment of the success or failure of cell therapy treatments.

## References

- Fodor WL. Tissue engineering and cell based therapies, from the bench to the clinic: the potential to replace, repair and regenerate. *Reprod Biol Endocrinol* 2003;1:102-7.
- Bexell D, Scheduling S, Bengzon J. Toward brain tumor gene therapy using multipotent mesenchymal stromal cell vectors. *Mol Ther* 2010;18:1067-75.
- Cashman TJ, Gouon-Evans V, Costa KD. Mesenchymal stem cells for cardiac therapy: practical challenges and potential mechanisms. *Stem Cell Rev* 2013;9:254-65.
- Ichim TE, Alexandrescu DT, Solano F, Lara F, Campion RDN, Paris E, et al. Mesenchymal stem cells as anti-inflammatories: implications for treatment of Duchenne muscular dystrophy. *Cell Immunol* 2010;260:75-82.
- Uccelli A, Laroni A, Freedman MS. Mesenchymal stem cells for the treatment of multiple sclerosis and other neurological diseases. *Lancet Neurol* 2011;10:649-56.
- Nguyen PK, Nag D, Wu JC. Methods to assess stem cell lineage, fate and function. *Adv Drug Deliv Rev* 2010;62:1175-86.
- Meyer GP, Wollert KC, Drexler H. Stem cell therapy: a new perspective in the treatment of patients with acute myocardial infarction. *Med Res* 2006;11:439-46.
- Wang Y, Xu C, Ow H. Commercial nanoparticles for stem cell labeling and tracking. *Theranostics* 2013;3:544-60.
- Janowski M, Bulte JWM, Walczak P. Personalized nanomedicine advancements for stem cell tracking. *Adv Drug Deliv Rev* 2012;64:1488-507.
- Srivastava AK, Bulte JWM. Seeing stem cells at work in vivo. *Stem Cell Rev* 2014;10:127-44.
- Bongso A, Fong C-Y, Gauthaman K. Taking stem cells to the clinic: major challenges. *J Cell Biochem* 2008;105:1352-60.
- Tong L, Zhao H, He Z, Li Z. Current perspectives on molecular imaging for tracking stem cell therapy. In: Okechukwu FE, editor. *Med. Imaging*; 2013.
- Aamtzen EHJG, Srinivas M, Walczak P, Janowski M, Heerschap A, de Vries IJM, et al. In vivo tracking techniques for cellular regeneration, replacement, and redirection. *J Nucl Med* 2012;53:1825-8.
- Ankri R, Taitelbaum H, Fixler D. On phantom experiments of the photon migration model in tissues. *Open Opt J* 2011;5:28-32.

15. Fixler D, Garcia J, Zalevsky Z, Weiss A, Deutsch M. Pattern projection for subpixel resolved imaging in microscopy. *Micron* 2007; **38**:115-20.
16. Ruan J, Ji J, Song H, Qian Q, Wang K, Wang C, et al. Fluorescent magnetic nanoparticle-labeled mesenchymal stem cells for targeted imaging and hyperthermia therapy of in vivo gastric cancer. *Nanoscale Res Lett* 2012; **7**:309-21.
17. Nam SY, Ricles LM, Suggs LJ, Emelianov SY. In vivo ultrasound and photoacoustic monitoring of mesenchymal stem cells labeled with gold nanotracers. *PLoS One* 2012; **7**:e37267.
18. Bhatnagara P, Li Z, Choi Y, Guo J, Li F, Lee DY, et al. Imaging of genetically engineered T cells by PET using gold nanoparticles complexed to Cooper-64. *Integr Biol (Camb)* 2014; **5**:231-8.
19. Ahrens ET, Bulte JWM. Tracking immune cells in vivo using magnetic resonance imaging. *Nat Rev Immunol* 2013; **13**:755-63.
20. Walter GA, Cahill KS, Huard J, Feng H, Douglas T, Sweeney HL, et al. Noninvasive monitoring of stem cell transfer for muscle disorders. *Magn Reson Med* 2004; **51**:273-7.
21. Meir R, Shamalov K, Betzer O, Motiei M, Horovitz-Fried M, Yehuda R, et al. Nanomedicine for cancer immunotherapy: tracking cancer-specific T-cells in vivo with gold nanoparticles and CT imaging. *ACS Nano* 2015; **9**:6363-72.
22. Betzer O, Shwartz A, Motiei M, Kazimirsky G, Gispan I, Damti E, et al. Nanoparticle-based CT imaging technique for longitudinal and quantitative stem cell tracking within the brain: application in neuropsychiatric disorders. *ACS Nano* 2014; **8**:9274-85.
23. Betzer O, Meir R, Dreifuss T, Shamalov K, Motiei M, Shwartz A, et al. In-vitro optimization of nanoparticle-cell labeling protocols for in-vivo cell tracking applications. *Sci Rep* 2015; **5**:15400-11.
24. Cho EC, Zhang Q, Xia Y. The effect of sedimentation and diffusion on cellular uptake of gold nanoparticles. *Nat Nanotechnol* 2011; **6**:385-91.
25. Chithrani BD, Ghazani AA, Chan WCW. Determining the size and shape dependence of gold nanoparticle uptake into mammalian cells. *Nano Lett* 2006; **6**:662-8.
26. Chithrani BD, Stewart J, Allen C, Jaffray DA. Intracellular uptake, transport, and processing of nanostructures in cancer cells. *Nanomedicine* 2009; **5**:118-27.
27. Khan MS, Vishakante GD, Siddaramaiah H. Gold nanoparticles: a paradigm shift in biomedical applications. *Adv Colloid Interface Sci* 2013; **199-200**:44-58.
28. Bao C, Conde J, Polo E, del Pino P, Moros M, Baptista PV, et al. A promising road with challenges: where are gold nanoparticles in translational research? *Nanomedicine (Lond)* 2014; **9**:2353-70.
29. Liu Y, Yang M, Zhang J, Zhi X, Li C, Zhang C, et al. Human induced pluripotent stem cells for tumor targeted delivery of gold nanorods and enhanced Photothermal therapy. *ACS Nano* 2016; **10**:2375-85.
30. Ricles LM, Nam SY, Sokolov K, Emelianov SY, Suggs LJ. Function of mesenchymal stem cells following loading of gold nanotracers. *Nanomedicine* 2011; **6**:407-16.
31. Astolfo A, Schültke E, Menk RH, Kirch RD, Juurlink BJJ, Hall C, et al. In vivo visualization of gold-loaded cells in mice using x-ray computed tomography. *Nanomedicine* 2013; **9**:284-92.
32. Long CM, Alric C, Tillement O, Link TW. Trimodal gadolinium-gold pancreatic islet cells restore Normoglycemia in diabetic mice and can be tracked by using US, purpose: methods: results. 2011; **260**:790-8.
33. Jokerst JV, Thangaraj M, Kempen PJ, Sinclair R, Sanjiv S. Photoacoustic imaging of mesenchymal stem cells in living mice via silica-coated gold nanorods. *ACS Nano* 2013; **6**:5920-30.
34. Ankri R, Ashkenazy A, Milstein Y, Brami Y, Olshinka A, Goldenberg-Cohen N, et al. Gold Nanorods based air scanning electron microscopy and diffusion reflection imaging for mapping tumor margins in squamous cell carcinoma. *ACS Nano* 2016; **10**:2349-56.
35. Ota S, Uehara K, Nozaki M, Kobayashi T, Terada S, Tobita K, et al. Intramuscular transplantation of muscle-derived stem cells accelerates skeletal muscle healing after contusion injury via enhancement of angiogenesis. *Sports Med* 2011; **39**:1912-22.
36. Wang P, Zhang Y, Zhao J, Jiang B. Intramuscular injection of bone marrow mesenchymal stem cells with small gap neurotaphy for peripheral nerve repair. *Neurosci Lett* 2015; **585**:119-25.
37. Garrovo C, Bergamin N, Bates D, Cesselli D, Beltrami AP, Lorenzon A, et al. In vivo tracking of murine adipose tissue-derived multipotent adult stem cells and ex vivo cross-validation. *Mol Imaging* 2013; **2013**:426961-73.
38. Enustun BV, Turkevich J. Coagulation of colloidal gold. *J Am Chem Soc* 1963; **85**:3317-28.
39. Feldkamp LA, Davis LC, Kress JW. Practical cone-beam algorithm. *J Opt Soc Am A* 1984; **1**:612.
40. Yan G, Tian J, Zhu S, Dai Y, Qin C. Fast cone-beam CT image reconstruction using GPU hardware. *J Xray Sci Technol* 2008; **16**:225-34.
41. Lee HK, Finnis S, Cazacu S, Xiang C, Brodie C. Mesenchymal stem cells deliver exogenous miRNAs to neural cells and induce their differentiation and glutamate transporter expression. *Stem Cells Dev* 2014; **23**:2851-61.
42. Lee HK, Finnis S, Cazacu S, Bucris E, Ziv-Av A, Xiang C, et al. Mesenchymal stem cells deliver synthetic microRNA mimics to glioma cells and glioma stem cells and inhibit their cell migration and self-renewal. *Oncotarget* 2013; **4**:346-61.
43. Markert CD, Atala A, Cann JK, Christ G, Furth M, Ambrosio F, et al. Mesenchymal stem cells: emerging therapy for Duchenne muscular dystrophy. *PM R* 2009; **1**:547-59.
44. Wada E, et al. In: Hegde M, editor. *Muscular Dystrophy*. InTech; 2012.
45. Kikkawa N, et al. Ectopic calcification is caused by elevated levels of serum inorganic phosphate in mdx mice. *Cell Struct Funct* 2009; **34**:77-88.